MAUSAM, **76**, 3 (July, 2025), 934-941

MAUSAM

DOI : https://doi.org/10.54302/mausam.v76i3.6220
Homepage: https://mausamjournal.imd.gov.in/index.php/MAUSAM

UDC No.551.577.1(541)

Dynamics of Orographic Rainfall for mountain corner over north-east India

PRASANTA DAS[1]* and SOMENATH DUTTA[2]

[1]*Department of Mathematics, Ramananda College, Bishnupur, Bankura, W.B., India*

[2]*India Meteorological Department (IMD), Pune, India* (**dutta.drsomenath@gmail.com**.)

(Received 05 April 2023, Accepted 09 May 2025).

***Corresponding author's email: pdas.math1986@gmail.com**

सार– उत्तर-पूर्व भारत में, कॉर्नर माउंटेन लगभग समकोण कोना है, जो खासी-जयंतिया पहाड़ियों (KJH) और असम-बर्मा पहाड़ियों (ABH) के बीच बना है। इस शोधपत्र में, एक दाब प्रवणिक माध्य प्रवाह में, भारत के उत्तर-पूर्वी क्षेत्र में दक्षिण-पश्चिम मॉनसून ऋतु (SWMS) के दौरान पर्वतीय वर्षा के प्रभावों का विश्लेषण किया गया। इस मॉडल के निर्माण के लिए 3-डी स्तरीय, गैर-चिपचिपा, रुद्धोष्म, बौसिनेसक और गैर घूर्णी नम वायु प्रवाह पर विचार किया गया। मूल प्रवाह के दो घटक हैं, कटिबंधीय पवन U(z) और रेखांशिक पवन V(z) और ब्रंट-वैसला आवृत्ति (N) को ऊंचाई से परिवर्त माना जाता है। वायु प्रवाह के गैर-रैखिक शासक समीकरणों को गड़बड़ी तकनीक का उपयोग करके रैखिक किया गया। वर्षा की तीव्रता (आरएफआई) की गणना करने के लिए, ऊर्ध्वाधर वेग () अर्ध-संख्यात्मक दृष्टिकोण से प्राप्त किया जाता है। इस अध्ययन में, दो चुनिंदा तिथियों पर विचार किया गया और सभी परिणामों की तुलना पहले के शोधकर्ताओं के परिणामों से की गई।

ABSTRACT. In north-east India, the Corner Mountain is an almost right angled corner, which is made between the Khasi-Jayantia hills (KJH) & the Assam-Burma hills (ABH). In this paper, has been made to analysis the effects of orographic rainfall during the south west monsoon season (SWMS) over the north-east region of India, in a baroclinic mean flow. To construct this model a 3-D laminar, non-viscous, adiabatic, Boussinesq & non rotational moist airflow has been considered. The basic flow has two components, zonal wind U(z) and meridional wind V(z) and the Brunt-Väisälä frequency (N) is taken to be variant with height. The non-linear governing equations of the airflow are linearized by using the perturbation technique. To compute the rainfall intensity (RFI), the vertical velocity ( ) is obtained by quasi-numerical approach. In this study, two selective dates has been considered and all results have compared to the earlier researchers.

Keywords – RFI, CMH, SWMS, Gridded rainfall data.

1. Introduction

The presence of an orographic barrier in any region considerably affects its rainfall patterns in terms of intensity & distribution. The distribution of rainfall is significantly influenced by the forced orographic uplift of unsaturated air, which leads to condensation & precipitation. In India, the geographical location of mountain barriers plays a crucial role in the spatial distribution of rainfall during the SWMS. The physical phenomenon of the precipitation is, the air is chilled beyond its saturation stage and it can no longer hold all the water vapour in the gaseous phase then it condenses as a cloud and finally come to the ground as a rain (Ludlam, 1956).

The studies on the dynamics of orographic rainfall problem across different mountainous regions were addressed by Banerjee (1929,1930), Douglas and Glasspoole (1947), Murray (1948), Sawyar (1956), Sarker(1966, 1967), De (1971), Smith (1979), Grossman and Duran (1984), Sinha Ray (1988), *etc*.

Banerjee (1929,1930) studied the effect of the mountain ranges on the configuration of the isobars & air motion. A note of rainfall over Cherrapunji in India developed by Murray (1948). Douglas and Glasspoole (1947) developed a heavy orographic rainfall model corresponding to the meteorological conditions across the British Isles. Sarker (1966, 1967) first developed a sound dynamical orographic rainfall model based on theories of airflow over mountains. The agreement between observed rainfall and his computed rainfall over the Western-Ghats during SWMS was remarkable. De (1971) observed the effect of mountain waves over northeast India and its neighbouring areas. Smith (1979) examined the influence of mountains on atmosphere. Grossman and Duran (1984) studied the interaction between low-level flow & Western - Ghats mountains in the summer monsoon season. Sinha

Ray (1988) examined two-dimensional effects of orography on airflow & rainfall across the mountain regions.

Dutta*et al*. (2006) observed the dynamic role of Western-Ghats to enhancement of RFI over Pune in India during SWMS. They also examined the effect of the Palghat gap on the RFI during SWMS and displayed that the perturbation of vertical velocity decreases with height at Palghat gap. Dutta *et al*. (2006) developed a 3-D dynamical model to study orographic rainfall over the WG during SWMS. The model consisted of two components: a dynamical part and a thermodynamical part. In the thermodynamical section, RFI was calculated using vertical velocity. The effect of static stability above the upper boundary on orographic rainfall was further examined by Dutta (2016).

Das *et al*. (2017) developed a 3-D dynamical model of lee wave across the Corner Mountain in the northeast region of India. They considered the two basic flow components, zonal wind (U) and meridional wind (V) variant with height. Das *et al.* (2018) used a three-dimensional model of rainfall developed by Dutta (2006), over the ABH during SWMS. They compared their computed RFI with observed RFI as well as with that computed by a 2-D model. They also studied the effect of the valley on rainfall intensity over ABH.

In the northeast region of India, the ABH is broadly north-south oriented whereas the KJH is broadly east-west oriented and they meet at almost a right angle, and forming a mountain corner. It is observed that the RFI in that region is not solely influenced by the KJH or the ABH individually, rather it is influenced by their combined effect. To study the problem of this combined effect, one has to investigate the effect of the above mountain corner on rainfall in that region.

From the foregoing discussions, it appears that the effect of the mountain corner on orographic rainfall associated with moist airflow in the northeast region of India, is not addressed so far. So, in our current study, a 3-D dynamical orographic model is developed to parameterize the orographic RFI over the northeast region in India during SWMS and finally, the computed results have been analogized to the observed rainfall data.

2. Data and methodology

2.1. *Database*

Guwahati (26.19º N Latitude and 91.73º E Longitude) is the only Radio Sonde station to the upstream of ABH and KJH. Accordingly, for the present study the average of 0000UTC and 1200UTC RS/RW data of Guwahati for 25th July 2002 and 15th August 2003 have been used, which corresponds to the observed lee waves across ABH and high resolution (0.25X0.25 degree) Daily Gridded Rainfall Data (DGRD) set over India, obtained from Archive of IMD, Pune, India, have also been used.

2.2. *Methodology*

In this model, all physical conditions and physical phenomenon are same as Das and Dutta (2022). Similar to Das and Dutta (2022), the Brunt-Väisälä frequency (N) and both components U,V are changing with vertical. A co-ordinate system, *x*-axis along U, *y*-axis along V and vertically z-axis is considered. Using the similar technique by Das and Dutta (2022), we have a vertical structure equation:

$$\frac{\partial^2 \hat{w}_1}{\partial z^2} + \left\{ f(k,l,z) - K^2 \right\} \hat{w}_1 = 0 \qquad (1)$$

$$f(k,l,z) = \frac{N^2(k^2+l^2)}{(kU+lV)^2} - \left(\frac{k\frac{dU}{dz}+l\frac{dV}{dz}}{kU+lV} \right) \frac{1}{\rho_0} \frac{\mathrm{d}\rho_0}{\mathrm{d}z} - \left(\frac{k\frac{d^2U}{dz^2}+l\frac{d^2V}{dz^2}}{kU+lV} \right) + \frac{1}{4\rho_0^2}\left(\frac{d\rho_0}{dz}\right)^2 - \frac{1}{2\rho_0}\frac{d^2\rho_0}{dz^2} \qquad (2)$$

where $N = \sqrt{\frac{g}{\theta_0}\frac{d\theta_0}{dz}}$ is the Brunt-Vaisala frequency and $K^2 = k^2 + l^2$.

The solution of Eqn. (1) is completely dependent on the value of $f(k,l,z)$. Similar to Das *et al.* (2016, 2018, 2022), Dutta (2005, 2007), Sarker (1966, 1967) and Palm and Foldvik (1960), it is assumed that $f(k,l,z) = 0$ at the maximum height. Let us take the approximate solution of Eqn. (1) for $f(k,l,z) = 0$ is

$$\hat{w}_1(k,l,z) = Ce^{-Kz} \qquad (3)$$

where *C* is constant and $\hat{w}_1$, $\frac{\partial^2 \hat{w}_1}{\partial z^2}$ are continuous function of z when $f(k,l,z) = 0$. Therefore,

$$\frac{\partial \hat{w}_1}{\partial z} = -K\hat{w}_1 \qquad (4)$$

Now, the equations (3) and (4) represent the upper boundary conditions of the Eqn. (1). The image of CMH is depicted in Fig. 1 and is analytically expressed as:

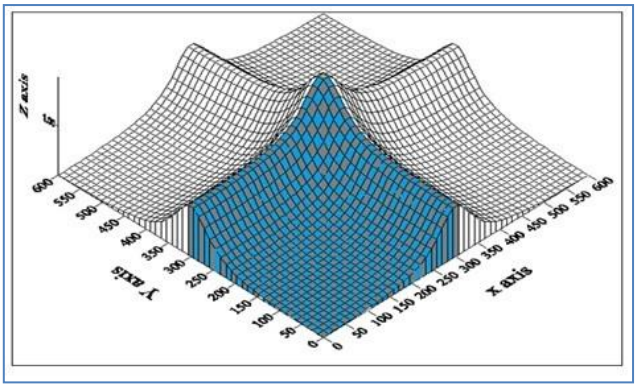

Fig. 1. Profile of the Corner Mountain Hills

$$h(x,y)=\frac{H}{2}\left[\frac{a^2}{a^2+(x-x_0)^2}+\frac{b^2}{b^2+(y-y_0)^2}\right] \quad (5)$$

Here the Blue and Gray colour is our study area. Now the values of parameters *H=2km*, *a=50km*, *b=50km*, x_0 *=300km* and y_0 =300km have been considered. If $\hat{h}(k,\ l)$ be the 2-D Fourier transformation of $h(x,y)$. Therefore,

$$\hat{h}(k,l)=-\frac{iH}{2}\left[\frac{a}{l}e^{-ak-ikx_0}+\frac{b}{k}e^{-bk-ily_0}\right] \quad (6)$$

Let us consider an arbitrary function $\phi(k,l,z)$, satisfies the Eqn. (1) and the boundary conditions (3) and (4) at $z=z_1=n\,d$. Therefore,

$$\frac{\partial^2\phi}{\partial z^2}+\left\{f(k,l,z)-K^2\right\}\phi=0 \quad (7)$$

$$\frac{\partial\phi}{\partial z}=-K\phi \quad (8)$$

We consider $\phi(k,l,nd)=1$ [Das *et al.* (2018)]. Here both $\phi(k,l,z)$ and $\hat{w}_1(k,l,z)$ are satisfying the following equation.

$$\frac{\partial^2\eta}{\partial z^2}+\left\{f(k,l,z)-K^2\right\}\eta=0 \quad (9)$$

Now, the Wronskian of $\hat{w}_1$ an ϕ at $z=z_1=n\,d$ is

$$W(\hat{w}_1,\phi,z)=\left|\begin{matrix}\hat{w}_1 & \phi\\ \frac{\partial\hat{w}_1}{\partial z} & \frac{\partial\phi}{\partial z}\end{matrix}\right|_{z=z_1}=\hat{w}_1(k,l,z_1)\frac{\partial\phi(k,l,z_1)}{\partial z}-\phi(k,l,z_1)\frac{\partial\hat{w}_1(k,l,z_1)}{\partial z}=0$$

The Wronskian result shows that both $\emptyset(k,l,z)$ and $\hat{w}_1(k,l,z)$are linearly dependent solutions of the Eqn. (9) at $z=z_1=n\,d$. So $\hat{w}_1(k,l,z)$ can be expressed as following:

$$\hat{w}_1(k,l,z)=B\phi(k,l,z)\text{ at }0\le z\le z_1 \quad (10)$$

where *B* is any constant and at $z=0$(at lower boundary condition), w'_1 is given by

$$w'_1(x,y,0)=w'(x,y,0)=U(0)\frac{\partial h(x,y,0)}{\partial x}+V(0)\frac{\partial h(x,y,0)}{\partial y}$$

With the application of Fourier double transformation of the above equation, it becomes

$$\hat{w}_1(k,l,0)=i\left\{kU(0)+lV(0)\right\}\hat{h}(k,l) \quad (11)$$

Using same procedure of Das *et al.* (2016, 2018) and using (11), the constant *B* is evaluated. Then $\hat{w}_1(k,l,z)$ can be represented as

$$\hat{w}_1(k,l,z)=i\left\{kU(0)+lV(0)\right\}\hat{h}(k,l)\frac{\phi(k,l,z)}{\phi(k,l,0)} \quad (12)$$

Therefore,

$$\hat{w}(k,l,z)=\sqrt{\frac{\rho_0(0)}{\rho_0(z)}}i\left\{kU(0)+lV(0)\right\}\hat{h}(k,l)\frac{\phi(k,l,z)}{\phi(k,l,0)} \quad (13)$$

Similar to Das *et al.* (2015, 2018) and Dutta (2007), the Eqn. (13) has been transformed to perturbation vertical velocity $w'(x,y,z)$ [using the inverse double Fourier transformation], then

$$w'(x,y,z)=\sqrt{\frac{\rho_0(0)}{\rho_0(z)}}\,\mathrm{Re}\left[\int_0^\infty\int_0^\infty i\left\{kU(0)+lV(0)\right\}\hat{h}(k,l)\frac{\phi(k,l,z)}{\phi(k,l,0)}e^{i(kx+ly)}\,dk\,dl\right] \quad (14)$$

In this paper, ignoring the earth's rotation in tropics, $\hat{h}(k,l)$ and $\emptyset(k,l,z)$ have been obtained numerically at (n+1) mesh point levels which is separated by the distance of $d=0.25$ km, for $l=-20\Delta l\ to-4\Delta l$ and $4\Delta l\ to\ 20\Delta l$, and $k=4\Delta k\ to\ 20\Delta k$, then the velocity $w'(x,y,z)$ is evaluated by the double integral formula in (14) numerically; where $\Delta k=\Delta l=\frac{2\pi}{4L_{max}}$ and L_{max} = 150 km is the maximum horizontal scale of the perturbation for horizontal speed wind of 10 ms^{-1}

[Dutta (2007)]. The horizontal perturbation scale should not beyond 150 km.

For the computation of orographic rainfall, the velocity $w'(x,y,z)$ is used. Similar to Dutta (2007) and Das *et al*. (2018), a unit cross-section air-column with top at $z = z_{i+1}$ and bottom $z = z_i$ is taken. So, the rate of rainfall is [Das *et al*. (2018) and Dutta (2007)].

$$RFI = -\int_{z_i}^{z_{i+1}} \vec{\nabla}.(\rho q \vec{V}')\, dz \qquad (15)$$

At steady state level $-\frac{\partial \rho}{\partial t} = \vec{\nabla}.(\rho \vec{V}') = 0$ and $\vec{\nabla}.(\rho q \vec{V}') = \rho \vec{V}'.\vec{\nabla} q + q\vec{\nabla}.(\rho \vec{V}')$. Then Eqn. (15) becomes

$$RFI = -\int_{z_i}^{z_{i+1}} (\rho \vec{V}'.\vec{\nabla} q)\, dz \qquad (16)$$

Now the moisture is horizontally homogeneous has been assumed. Hence, the frequency of rain is [Das *et al*. (2018) and Dutta (2007)]

$$-\int_{z_i}^{z_{i+1}} \rho w' \frac{\partial q}{\partial z} dz = -\int_{z_i}^{z_{i+1}} \frac{\partial (q \rho w')}{\partial z} dz + \int_{z_i}^{z_{i+1}} q \frac{\partial (\rho w')}{\partial z} dz$$

$$= -\left(\rho_{0i} q_i w_i' - \rho_{0(i+1)} q_{i+1} w_{i+1}'\right) + q'\left(\rho_{0(i+1)} w_{i+1}' - \rho_{0i} w'\right)$$

$$= \left\{\rho_{0i} w_i'(q_i - q') + \rho_{0(i+1)} w_{i+1}'(q' - q_{i+1})\right\} \qquad (17)$$

If the expression of density be kg m^{-3}, mixing ratio be gm kg^{-1} & vertical velocity be cm sec^{-1}, then the RFI from $Z = Z_i$ to $Z = Z_{i+1}$ is

$$= 0.036\left[\rho_{0i} w_i'(q_i - q') + \rho_{0(i+1)} w_{i+1}'(q' - q_{i+1})\right] \text{mm hr}^{-1} \qquad (18)$$

3. Results and discussion

The formula (18) has been used to calculate the orographic RFI over and across the CMH. The parameters of the CMH are $a = 50\ km = b,\ H = 2\ km$ and $x_0 = 300\ km = y_0$ are taken. In this paper, the calculated RFI is demonstrated in the presence and absence of V component and compared to 0.25 X 0.25 degree high contrast Daily Gridded Rainfall Data (DGRD) set over India. However, for the sake of brevity, only two cases are discussed here. SWMS being the principal rainy season, the cases are considered from this season with one case each from the months of July and August.

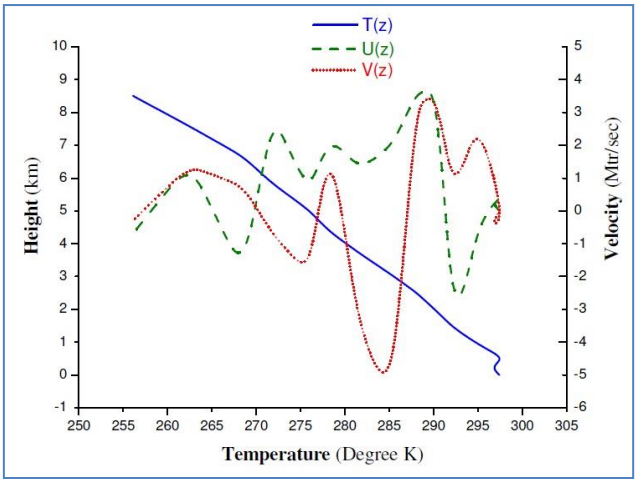

Fig. 2. Profile of U(z), V(z) and T(z) on 25.07.2002

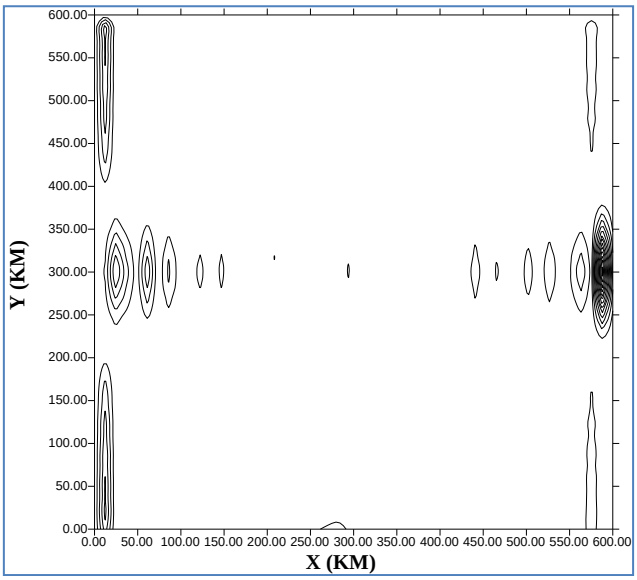

Fig. 3. Contour of RFI on 25.07.2002 when V absent

Case-I: 25th July 2002

RFI is calculated in the presence and absence of the V component across the CMH. The vertical profile of T(z), U(z) and V(z) are exhibited in Fig. 2. This shows that the temperature T(z) is approximated by a pseudo line which passes through the surface dry bulb temperature.

Using the profile above, the contours of calculated RFI on the plane are plotted in Fig. 3 when the V part is absent and Fig. 4 when the V part is exit.The four maximum RFI regions are seen when the V part is absent.

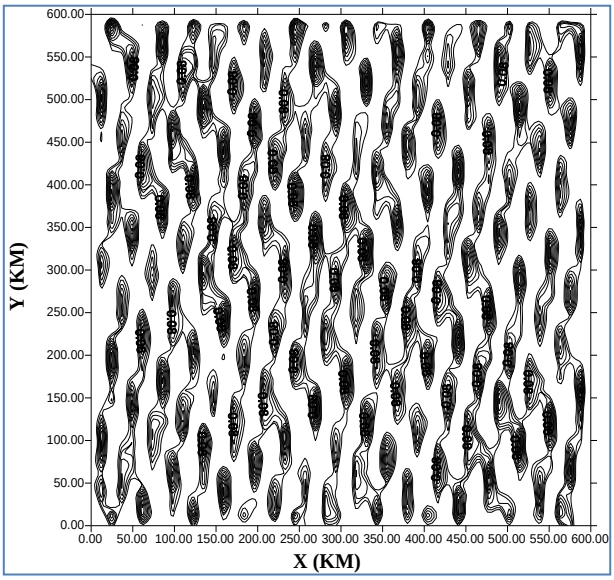

Fig. 4. Contour of RFI on 25.07.2002 when V exist

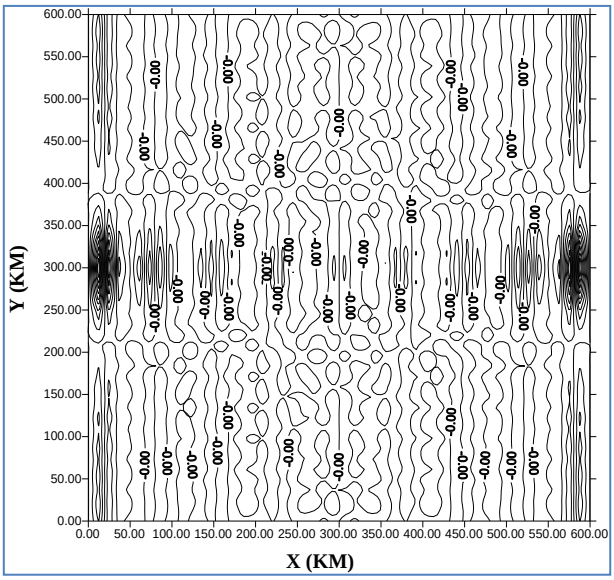

Fig. 5. Contour of w' on 25.07.2002 when V absent

The one primary maximum RFI is located between y = (300±85) km and at x = 600 km that is 300 km distance from the corner and on the leeward position of the CMH. The one secondary maxima RFI is occurred at x = 15 km to the windward position of the CMH between y = (300±65) km and the another two maximum RFI are placed uniformly near two edges of the barrier to the windward position beyond y = (300±100) km in Fig. 3.

If we observe the contours of perturbation vertical velocity w' when the V part is absent in Fig. 5, the position of maximum effected regions of w' are almost the same to the regions of maximum RFI in Fig. 3. In the existence

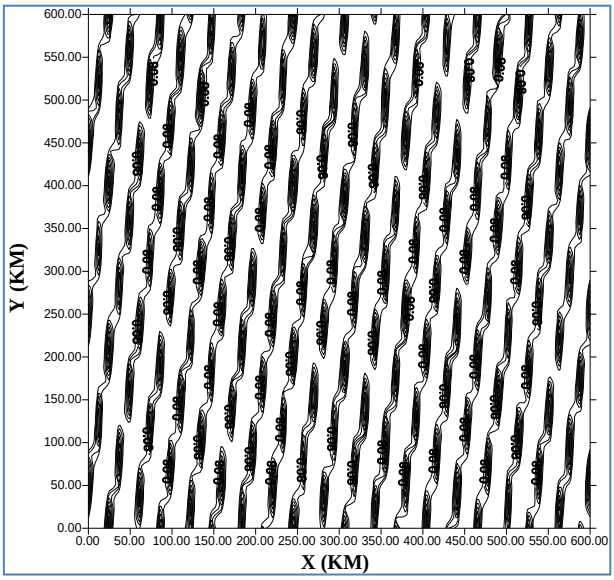

Fig. 6. Contour of w' on 25.07.2002 when V exist

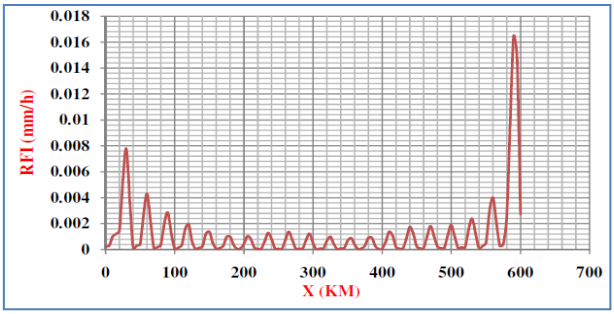

Fig. 7. Variation of RFI along y =300 on 25.07.2002 when V absent

of the V part, the contour of the calculated RFI on the plane is shown in Fig. 4. But, because of the existence of the V part there are no such particular fixed locations of the maximum RFI, which is in conformity to the contour pattern of w' in existence of the V part in Fig. 6.

In the absence of V component of winds, the distribution of the calculated RFI in the plane y = 300 (central plane) is depicted in Fig. 7. The maximum RFI in the plane y = 300 occurs on the leeward position of the corner (Peak) and the value of primary maximum RFI is 0.0164 mm hr^{-1} at x = 590 km that is 290 km distance from the corner position. The actual Gridded RFI for that date is 0.00 mm hr^{-1} at x = 575 km that is 275 km distance from the corner on the leeward position of CMH. The secondary maximum RFI is 0.0077 mm hr^{-1} at x = 30 kmto the windward position of the CMH.

In the presence of the V part, the calculated maximum RFI in the plane y=300 happens on the leeward position of the CMH in Fig. 8. The magnitude of the maximum RFI of that date is 0.114 mm hr^{-1} at x = 325 distance from the

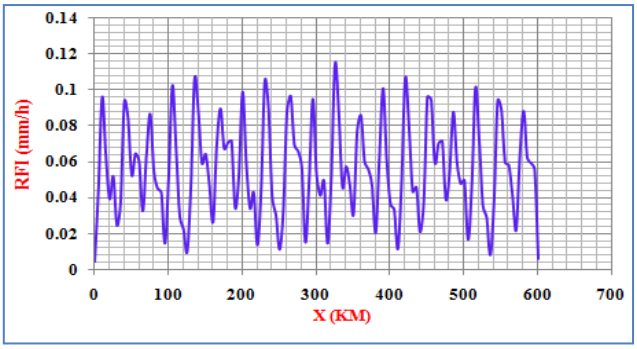

Fig. 8. Variation of RFI along y=300 on 25.07.2002 when V exist

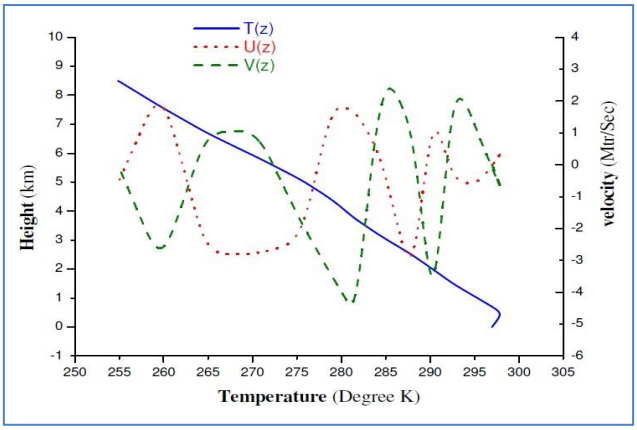

Fig. 9. Profile of U(z), V(z) and T(z) on 15.08.2003

corner (peak) to the leeward position of the CMH. There also so many additional RFI peaks are seen in Fig. 8, whereas no additional peak are seen when the V part is absent in Fig. 7.

Case-II: 15th August 2003

The profile of T(z), U(z) and V(z) of 15th August 2023 are depicted in Fig. 9. In this profile U(z) and V(z) are changing alternatively, positive and negative with height. During SWMS, the southerly movement across the CMH is indifferent corresponding to moist adiabatic lapse rate. So, the temperature T(z) is approximated by pseudo adiabatic through the surface dry bulb temperature.

Similar to Case-I, the contours of the calculated RFI on the plane y = 300 have been depicted in Fig. 10 and Fig. 11 when the V part is absent and present respectively. Fig. 10 shows four maxima RFI when the V component is present. Here the primary maximum one is situated at x = 580 km that is 280 km distance from the corner (Peak) and on the leeward position of the barrier between y = 380 km and y = 220 km. In other hand, the one secondary maximum RFI is seen at x = 25 km to the windward position of the CMH between y = 325 km and y = 275 km and two additional maximum RFI are happened uniformly near two edges of the barrier beyond y = (300 $\pm$ 100) km to the windward position of the CMH (Fig. 10). If we notice the contour of w' in Fig. 12, the maximum RFI regions are approximately the same to the contour of RFI in Fig. 10 when V is absent.

On other hand, when the V is present, the contour of calculated RFI is depicted in Fig. 11, where we have not found any specific fixed regions of maximum RFI. If we observe the contour of w' in Fig. 13 when the V part is exist, no such maximum effected regions are seen.

The distribution of the calculated RFI in the plane y = 300 is depicted in Fig. 14 when the V part is absent. This shows that the maximum RFI is at x = 588 km that is

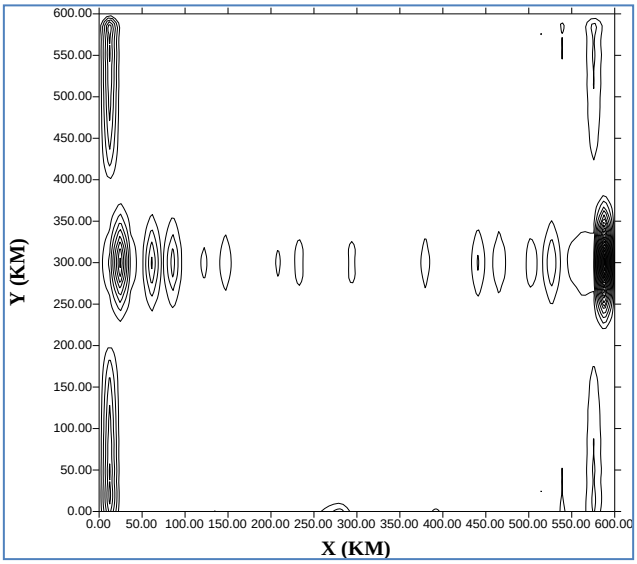

Fig.10. Contour of RFI on 15.08.2003 when V absent

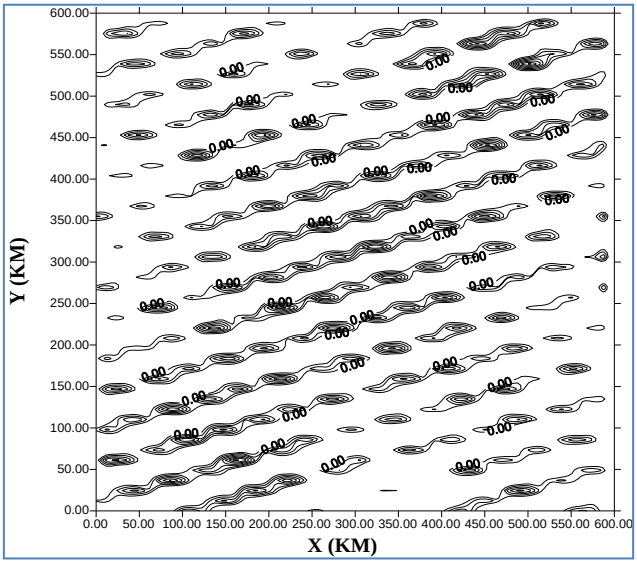

Fig. 11: Contour of RFI on 15.08.2003 when V exist

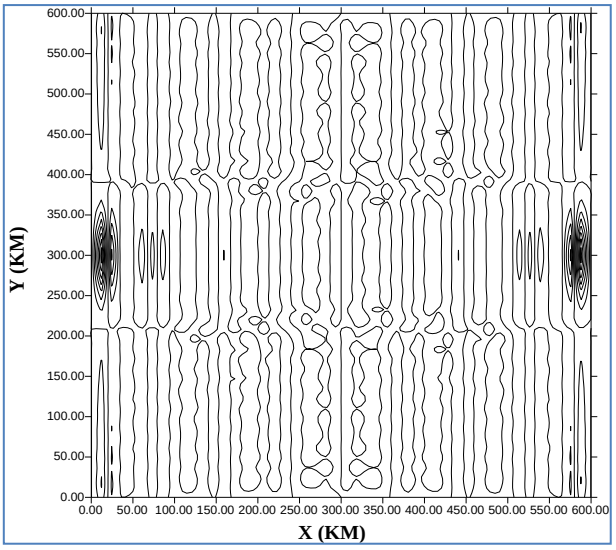

Fig. 12. Contour of w' on 15.08.2003 when V absent

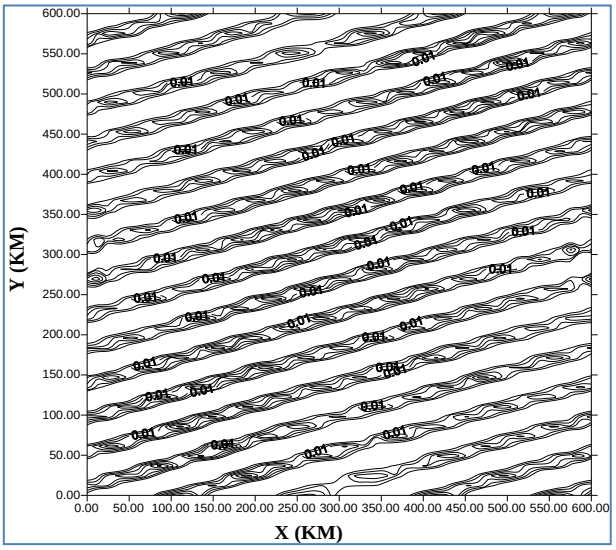

Fig. 13. Contour of w' on 15.08.2003 when V exist

288 km distance from the corner to the leeward position of the CMH and its magnitude 0.001154 mm h^{-1}. At that date, the Gridded RFI was 0.0 mm h^{-1} at x = 600 km that is 300 km distance from the corner to the leeward position of the CMH. The other secondary maximum RFI is 0.0045 mm h^{-1} at x = 25 kmto the windward position of the CMH.

In the existence of the V part, the distribution of RFI in the plane y = 300 has been shown in Fig. 15. Due to the existence of the V part, there is a one primary maximum RFI of magnitude 0.0048 mm h^{-1} at x = 260 kmon the windward position of the CMH and three additional multi peaks of magnitudes 0.0047, 0.0036 and 0.0033 mm h^{-1} at x = 405 km, x = 113 km and x = 554 km respectively, are found. But, no additional peaks are found when the V part is absent in Fig. 14.

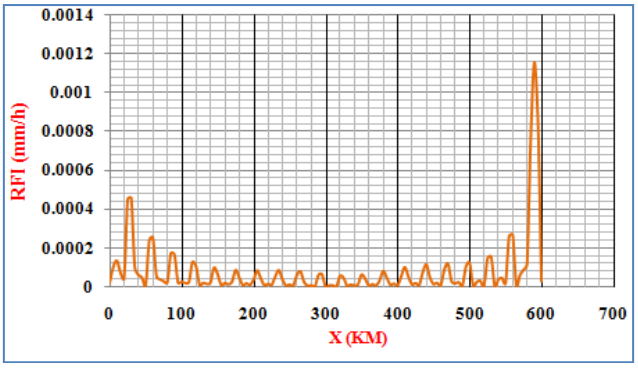

Fig. 14. Variation of RFI along y=300 on 15.08.2003 when V absent

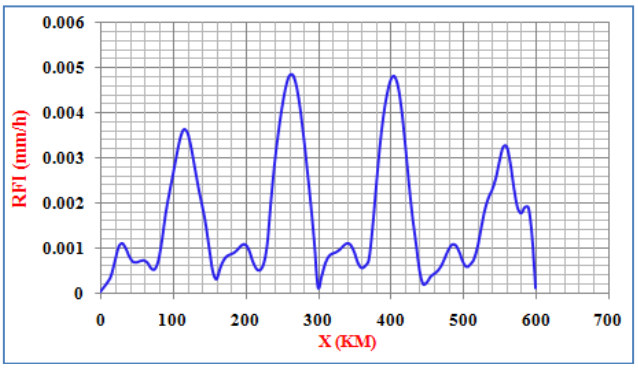

Fig. 15. Variation of RFI along y=300 on 15.08.2003 when V exist

4. Conclusions

In this study, a dynamical orographic rainfall model for 3-D lee wave across the CMH, has been presented. In an outcome, some remarkable observations have been made as following:

(*i*) In all cases, the maximum primary RFI occurs on the leeward position of the CMH and the secondary maximum RFI is happened in the windward position of the CMH.

(*ii*) It is more interesting that, the model position of the primary maximum RFI along $y = 300$ (central plane) is between 10 to 15 km to the Gridded position of the maximum RFI.

(*iii*) In both Case - I and Case - II, due to the absence of the V component, all the primary maximum RFI along the plane y = 300 are occurred between 280 km to 290 km to the leeward position of the peak (corner) and all the secondary maximum RFI occur between 25 km to 30 km to the windward position of the corner.

(*iv*) In the existence of the V part, for Case-I the primary maximum RFI along y = 300 is happened on the leeward position of the corner and for Case-II the primary maximum RFI is occurred to the windward position of the corner.

(*v*) In both Case-I and Case-II, a multi peaks RFI are found along y = 300 (central plane) when V is present, whereas no multi peaks are found when V is absent. In the absence of V part, all the primary maximum RFI occur to the leeward position of the corner and all the secondary maximum RFI are located uniformly about the plane y = 300 and they are equal in their magnitude. When V part is present, all the primary and secondary maximum RFI have lost the uniformity in pattern and unequal in their magnitude along y = 300.

(*vi*) In case CASE-I& II, we have seen that for a corner mountain, the primary maxima in the computed rainfall intensity occurs over the specific quadrant on the lee side and the secondary one occurs over the windward side. This result is contrary to the findings of Dutta (2007), where it was shown that for a three-dimensional mesoscale mountain with elliptical contour, the primary maxima of computed orographic rainfall intensity on the windward side and the secondary one on the lee side. Thus, the present study has been able to bring out the role of mountain shape or orientation in modulating the spatial distribution of orographic rainfall.

Acknowledgements

The author is grateful to Dr. U.S. De, Former Additional. Director General of Meteorology of India Meteorological Department and to Dr. G. Krishnakumar, Scientist-E, Head, National Data Centre, India Meteorological Department, Pune, Maharashtra, India and to Prof. M. Maiti, Retd. Professor and Prof. Shyamal Kumar Mandal, Department of Applied Mathematics with Oceanology and Computer Programming, Vidyasagar University, Midnapore, India for their kind valuable suggestions and guidance.

Authors' Contributions

Prasanta Das: Conceptualization, Methodology, Software, Validation, Formal analysis, Investigation, Writing-original draft.
Somenath Dutta : Conceptualization, Validation, Formal analysis, Investigation, Resources, Data curation, Writing - review & editing, Visualization, Supervision.

Disclaimer: The contents and views expressed in this research paper/article are the views of the authors and do not necessarily reflect the views of the organizations they belong to.

References

Banerjee, S. K. 1930, "The effect of Indian mountain ranges on air motion", *Ind. Jour. Phys*., **V**. 699 -745.

Banerjee, S. K. 1929, "The effect of the Indian mountain ranges on the configuration of the isobars", *Ind. Jour. Phys*., **IV**, 477-502.

Das P., Dutta S and Mondal S. K. 2016, "Momentum flux and energy flux associated with internal gravity waves excited by the Assam-Burma hills in India", *Modeling Earth Systems and Environment*. **2**, 2, 1-9.

Das P., Dutta S. and Mondal S. K. 2015, "A quasi-numerical solution for 3-D meso-scale lee wave associated with meso-scale baroclinic dry mean flow across the Assam-Burma hills in India", *J. Ind. Geophys. Union*.**19**, 3, 290-300.

DAS, P. and DUTTA, S., 2022, "A mathematical model for fluxes associated with internal gravity waves excited by a corner mountain", *MAUSAM*,**73**, 1, 181-188.

Das, P., Dutta, S. and Mondal, S. K., 2017, "A mathematical model for the 3-D dynamics of lee wave across a meso-scale mountain corner", *MAUSAM*, **68**, 2, 195-204.

Das, P., Dutta, S. and Mondal, S. K., 2018, "A dynamical model for diagnosing orographic rainfall across Assam-Burma hills in India. *Modeling Earth Systems and Environment", 4*, **4**, 1423-1433.

De U S. 1971, "Mountain waves over northeast India and neighbouring regions", *Indian journal of meteorology and geophysics*. 22**,** 361-364.

Douglas, C. K. M. andGlasspoole, J., 1947, "Meteorological conditions in heavy orographic rainfall in the British Isles",*Quarterly Journal of the Royal Meteorological Society*, **73**, 315-316, 11-42.

Dutta, S. 2005, "Effect of static stability on the pattern of 3-D baroclinic lee wave across a meso-scale elliptical barrier", *Meteorol Atmos Phys*, **90**, 139-152.

Dutta, S. N., Mukherjee A. K. and Singh A. K., 2006, "Effect of Palghat gap on the rainfall pattern to the north & south of its axis", *Mausam*, **57**, 4, 675.

Dutta, S., 2007, "Parameterization of momentum flux and energy flux associated with orographically excited internal gravity waves in a baroclinic background flow", *Mausam*, **58**, 4, 459-470.

Dutta, S., 2007, "A meso-scale three-dimensional dynamical model of orographic rainfall", *Meteorology and Atmospheric Physics*, 95, 1, 1-14.

Dutta, S., 2016, "Does the stability above the upper boundary have any effect on the orographic rainfall?", *Modeling Earth Systems and Environment*, **2**, 2, 1-11.

Dutta, S., Laskar, S. I. and Maiti, M., 2006, "Does the Western-Ghats play any dynamical role in the distance effect of vortex over the Bay of Bengal on the enhancement of monsoon rainfall over Pune?", *Mausam*, **57**, 4, 567-578.

Grossman, R. L. and Durran, D. R., 1984, "Interaction of low-level flow with the western Ghat Mountains and offshore convection in the summer monsoon", *Monthly Weather Review*, **112**, 4, 652-672.

Ludlam, F. H., 1956, "The structure of rainclouds", *Weather*.**11**,187-196.

Murray, 1948, "A note of rainfall of Cherrapunji", *Quart. Jour. Roy. Met.Soc*. **74**, 122-123.

Palm, E. and Foldvik, A. 1960, "Contribution to the theory of two-dimensional mountain waves", *Geo. Publ.*, **21**, 6, Oslo, 1-29.

Sarker, R. P. 1966, "A dynamical model of orographic rainfall", *Mon. Wea. Rev*.**94**, 555-572.

Sarker, R. P. 1967, "Some modifications in a Dynamical model of orographic rainfall. *Mon. Wea. Rev*.**95**, 673-684.

Sawyer, J. S., 1956, "The physical and dynamical problems of orographic rain. *Weather*, **11**, 12, 375-381.

Sinha, Ray K. C. 1988, "Some studies on effects of Orography on airflow and rainfall", Ph.D. thesis. *University of Pune, India*.

Smith, R. B., 1979, "The influence of mountains on the atmosphere", *Adv. Geophys*,**21**, 87-230.